Smart Rocks and Wireless Communication Systems for Real-Time Monitoring and Mitigation of Bridge Scour
(Progress Report No. 7)

Contract No: RITARS-11-H-MST
(Missouri University of Science and Technology)

Ending Period: April 15, 2013

PI: Genda Chen
Co-PIs: David Pommerenke and Y. Rosa Zheng

Program Manager: Mr. Caesar Singh

Submission Date: April 15, 2013

TABLE OF CONTENTS

EXECUTIVE SUMMARY 1

I - TECHNICAL STATUS 1

I.1 ACCOMPLISHMENTS BY MILESTONE 2

Task 1.1 Optimal Passive Smart Rock – Engineering design and validation of DC magnetic passive smart rocks 4

Task 1.2 Steel Interferences to Magnetic Measurements 8

Task 2.1 Active Smart Rocks with Embedded Controllable Magnets or with Embedded Electronics 9

Task 2.2(a) Magneto-Inductive Communications – Engineering design and validation of magneto-inductive transponders 12

Task 2.2(b) Acoustic Communications – Engineering evaluation of acoustic communication systems for bridge scour monitoring 12

Task 3.2 Field Validation Planning and Execution 14

I.2 PROBLEMS ENCOUNTERED 14

I.3 FUTURE PLANS 14

II – BUSINESS STATUS 17

II.1 HOURS/EFFORT EXPENDED 17

II.2 FUNDS EXPENDED AND COST SHARE 18

EXECUTIVE SUMMARY

In the seven quarter, field tests at two bridge sites continued to understand the long-term performance of both passive and active smart rocks deployed in late summer 2012. Emphasis was placed on additional characterization of prototype passive rocks, new development of controllable magnet active smart rock, additional design and implementation of circuitry for magnet flipping, and preliminary development of active rock localization schemes using intensity in magneto-inductive communication and phase difference in acoustic communication. In addition, the previous digital signal processing (DSP) algorithm was further investigated and expanded to realize a frequency demodulation from the 125 KHz carrier frequency to the baseband with 800 Hz bandwidth. Multiple acoustic sensing is also attempted.

For static magnetic field measurements, prototype passive rocks that were previously deployed and tested at bridge sites were used to develop a more accurate set of characteristics/calibration curves to relate the magnetic intensity to both measurement distance and magnet orientation. Prototypes with controllable magnets with applied current, referred to as active smart rocks, were also fabricated and demonstrated to be promising in laboratory. The present active rocks with controllabe magnets were made of an inner ball with one embedded magnet placed inside a sphere filled with high viscousity fluid between the ball and the sphere so that a “frictionless” interface can be created and the magnet can be flipped under current. Finally a coil was wrapped outside the sphere, with the designed circuitry, to flip the magnet as alternating current is supplied. In the following quarter, a new way of implementing controllable magnet active rocks with a gyroscope device will be designed and tested to further reduce the demand on the external power to flip magnet. In addition, field test data collected at bridge sites will be used to develop a localization algorithm based on the three measurements at three base stations.

For active smart rocks with magneto-inductive communication, low frequency receiver was used to increase the sensitivity of the proposed localization scheme based on the change in signal strength. The DSP algorithm was further developed with a frequency demodulating technique, converting the carrier frequency (125 KHz) to the baseband with a much low frequency bandwidth (800 Hz). The designed PCB board was modified and used to control magnets in the controllable magnet active rocks.

For active smart rocks with acoustic communication, both software and hardware were tested in a lake with two hydrophones placed near an acoustic projector. Results of the field tests indicated that the localization technique using phase difference worked very well. To improve the localization accuracy in field application, two sets of receivers, each with two receiving channels, will be used on two sides of a river. In this case, the time synchronization between multiple receivers becomes critical, which will be the main task of the next quarter. To combat acoustic reverberation, receiver equalization will also be implemented in the next quarter.

I - TECHNICAL STATUS

I.1 ACCOMPLISHMENTS BY MILESTONE

More measurements from laboratory tests of passive smart rocks and active smart rocks with magneto-inductive and acoustic communications were taken and analyzed in this quarter. In addition, controllable magnets were designed to create a new active smart rock for bridge scour monitoring.

Task 1.1 Optimal Passive Smart Rock – Engineering Design and Validation of DC Magnetic Passive Smart Rocks

Smart Rock Prototype Calibration: In an attempt to acquire cleaner characteristic behavior data from the prototype smart rock (4" in diameter), more tests were conducted with stronger control over the variables using a test apparatus. As a result, the characteristic behavior is more predictable and agrees with the equations relating magnetic intensity with distance from the magnet. Fig. 1(a-c) compares the overall trend of the orientation effect with respect to rotation about the respective axis as well as the distance between the magnet (smart rock) and the measuring device (magnetometer).

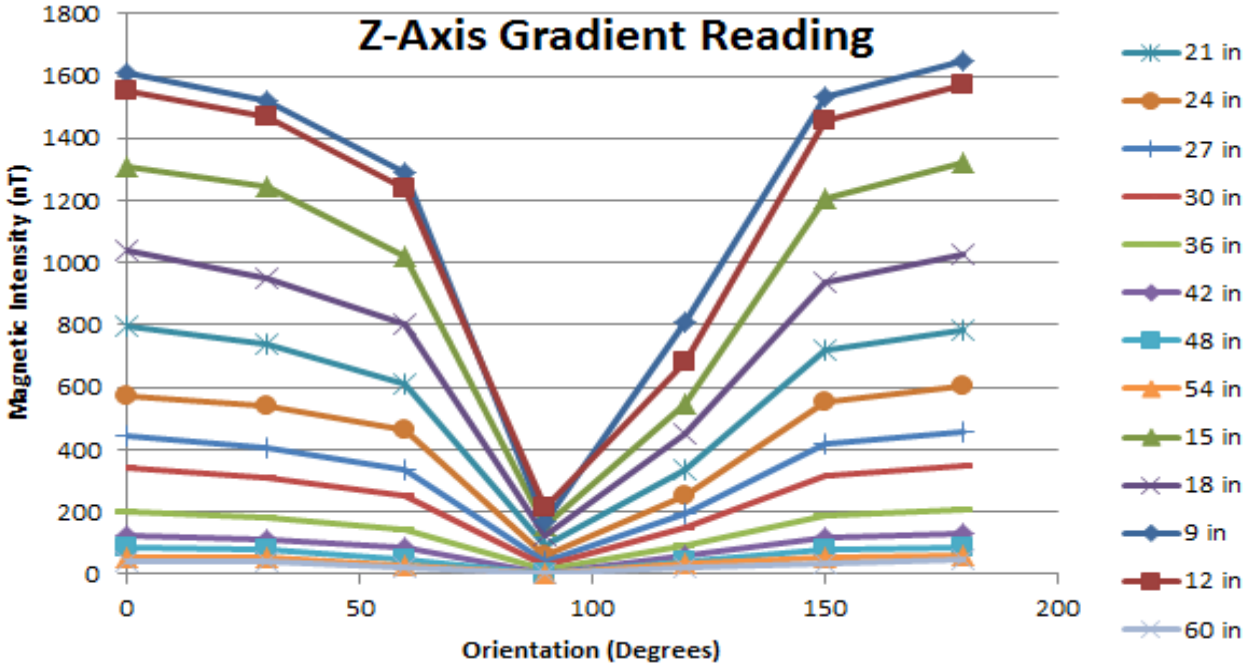

a) Rotation about Z-axis

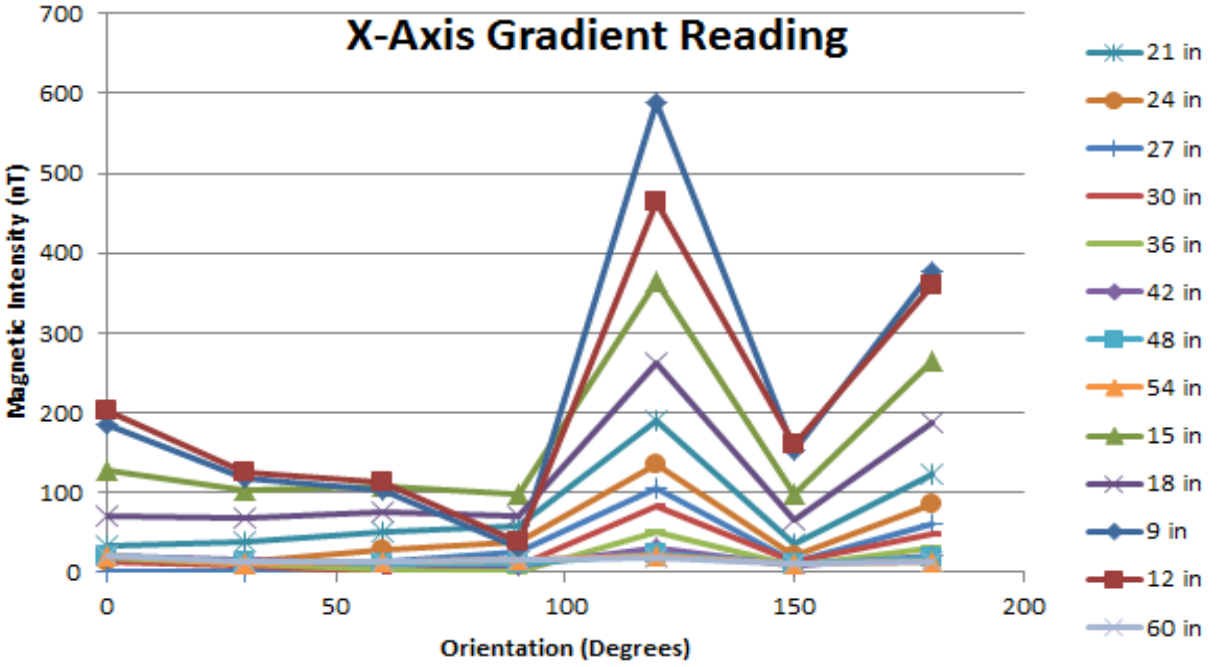

b) Rotation about X-axis

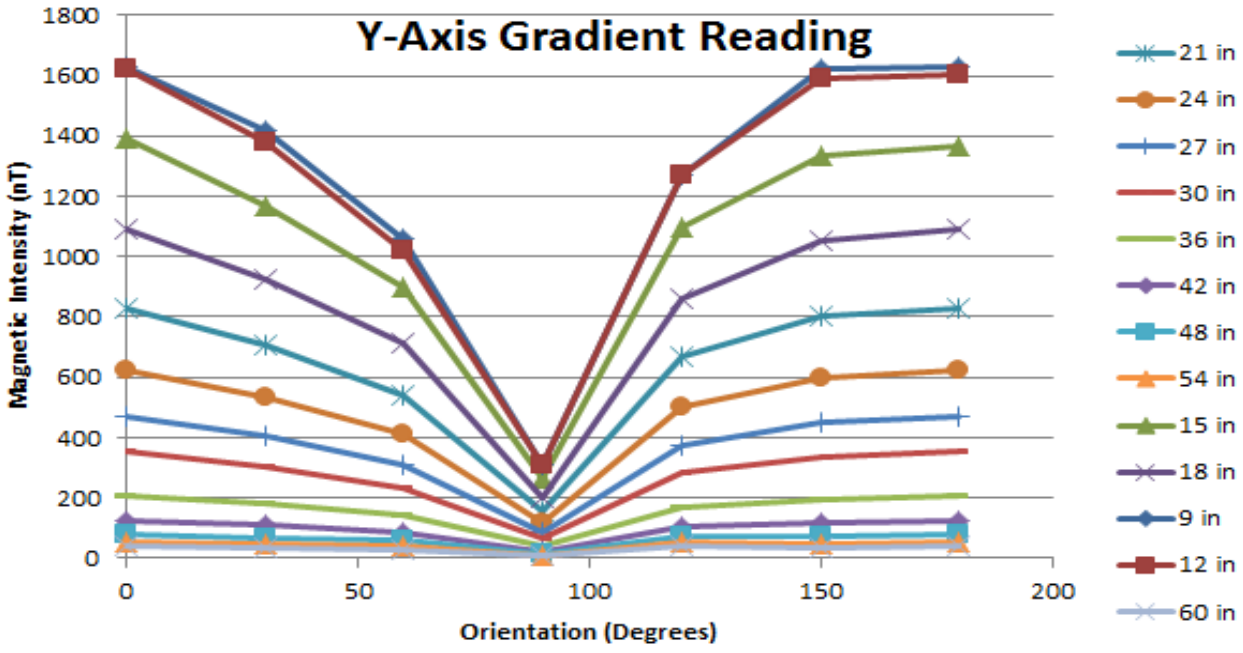

c) Rotation about Y-axis

Fig. 1 Comparison of the orientation effects along vertical distance changes

Alternatively, Fig. 2(a-c) compares the overall trend of the distance effect with respect to rotation about the respective axis as well as the orientation between the magnet (smart rock) and the measuring device (magnetometer). By fixing the orientation of the smart rock with respect to the magnetometer and varying the vertical distance between the two, cleaner intensity readings were recorded and plotted to emulate the natural trend of magnetic intensity as the distance increases when compared to the previous characteristic behavior calibrations discussed in the sixth report.

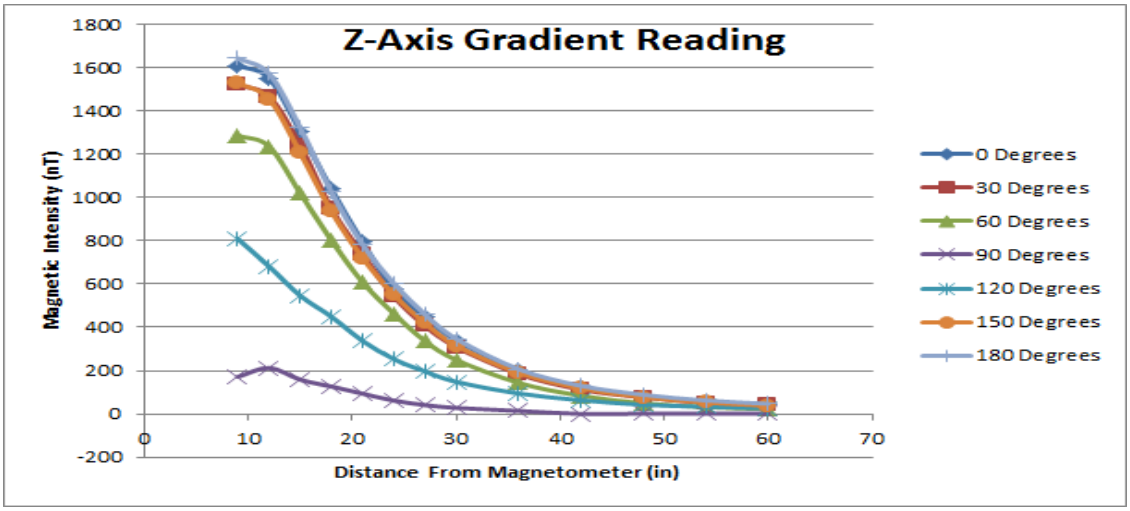

a) Rotation about Z-axis

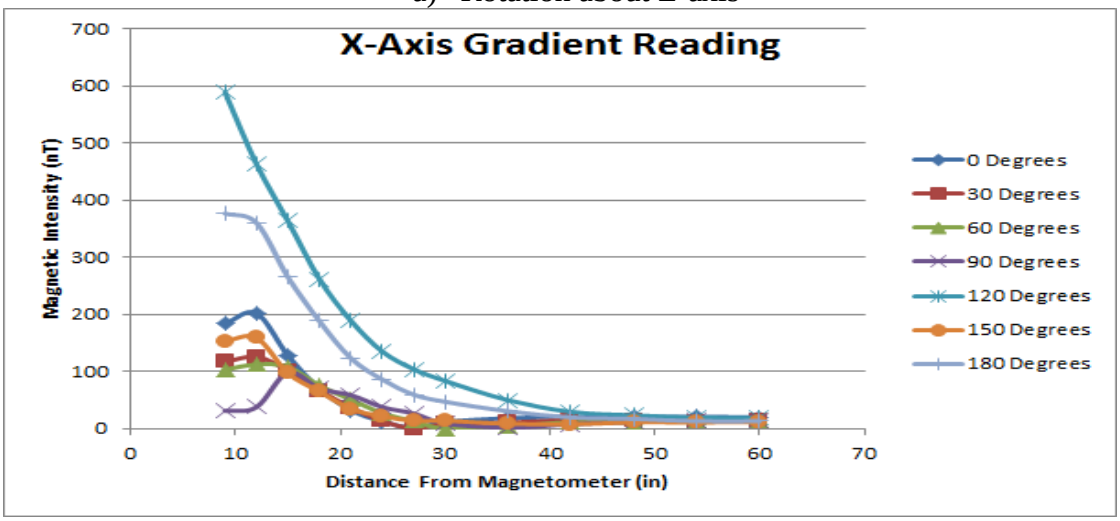

b) Rotation about X-axis

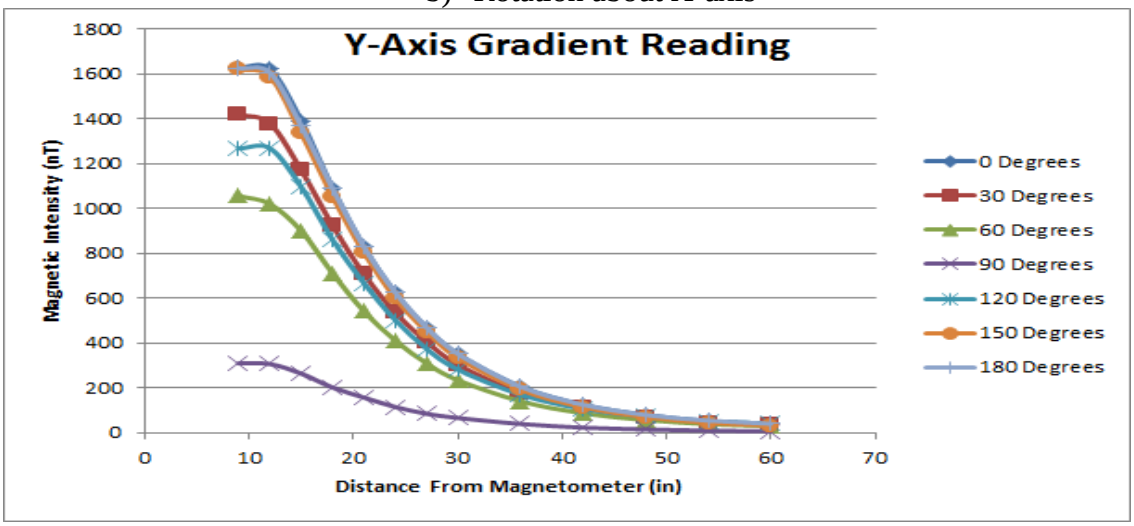

c) Rotation about Y-axis

Fig. 2 Comparison of the distance effect along smart rock orientation changes

Task 1.2 Steel Interferences to Magnetic Measurements – Noise Level, Data Cleansing and Engineering Interpretation with Passive Rocks Submitted

The previous report already indicated that the gradient measurement mainly removed the Earth's magnetic field. There is no clear sign of indication that the noise level in the gradient readings was reduced by the subtraction between the readings from two sensor heads of a magnetometer.

Task 2.1 Active Smart Rocks with Embedded Controllable Magnets or with Embedded Electronics – Engineering Design and Validation of Active Smart Rocks Submitted

In this quarter, a preliminary version of an active smart rock with controllable magnets has been developed and tested to determine the benefits and validity of the design. The proposed design was to suspend the passive smart rock with one magnet within a highly viscous liquid to approach frictionless conditions, Fig. 3. The passive rock was then wrapped within a coil that is subjected to alternating current, Fig. 4. By alternating the current, the magnet in the passive rock changes its polarization and flips without any external, physical manipulation.

Fig. 3 Passive smart rock suspended in silicone oil

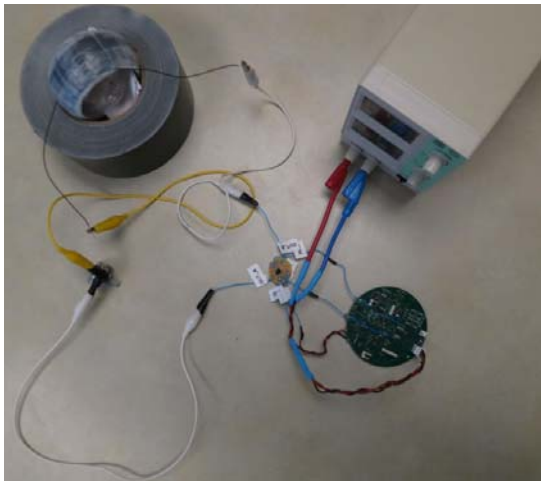

Fig. 4 Controllable magnet coil apparatus

Two active smart rocks were developed, ½"x1" magnet and $^{7}/_{16}$"x1" magnet, to observe the weight effect (remaining friction) of a larger smart rock. The test results verified that the effect of weight was negligible as the alternating current repetitively flipped both versions of the smart rock at the same power level.

To determine the effect of flipping the smart rock, a test matrix was developed. A continuous reading from the magnetometer (one reading every 0.1 seconds) was recorded for 30 seconds of flipping at ½' increments. These readings were then compared to a continuous 10 second reading of a stationary smart rock (without alternating current). Fig. 5 is a sample result of this comparison. Fig. 6 compares the effect of moving the magnetometer away from the smart rock. For clarity, only one foot increments are displayed on this graph.

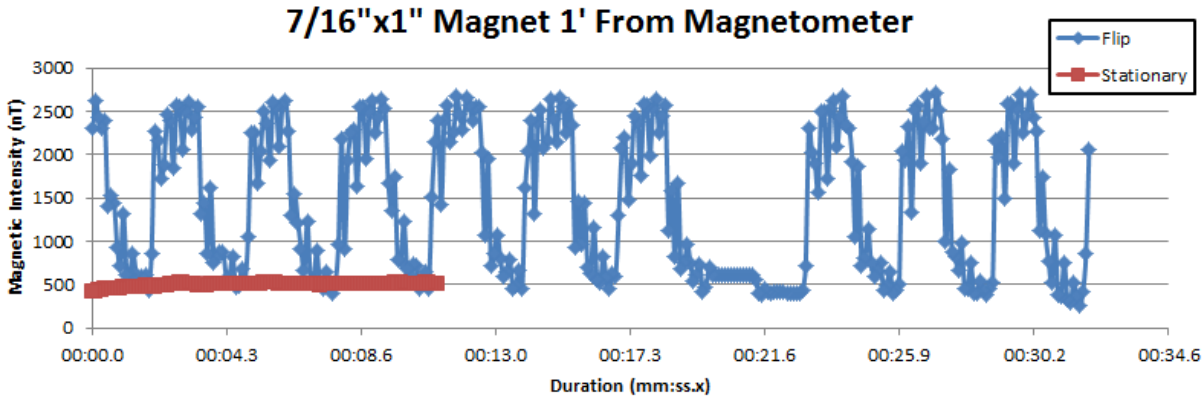

Fig. 5 Magnetic intensity of a flipping smart rock vs. a stationary smart rock

The implications of the preliminary results are promising. By implementing the active flipping effect of passive smart rocks, not only a correlation between distance and magnetic intensity but also a correlation between peak-to-peak distance and the distance from the magnetometer were received as shown in Fig. 6. With two correlating data relationships, the orientation as well as distance from the magnetometer may be determined with only one magnetometer location. This could potentially improve the inherent reliability of the magnetometer readings with respect to distance from the smart rock.

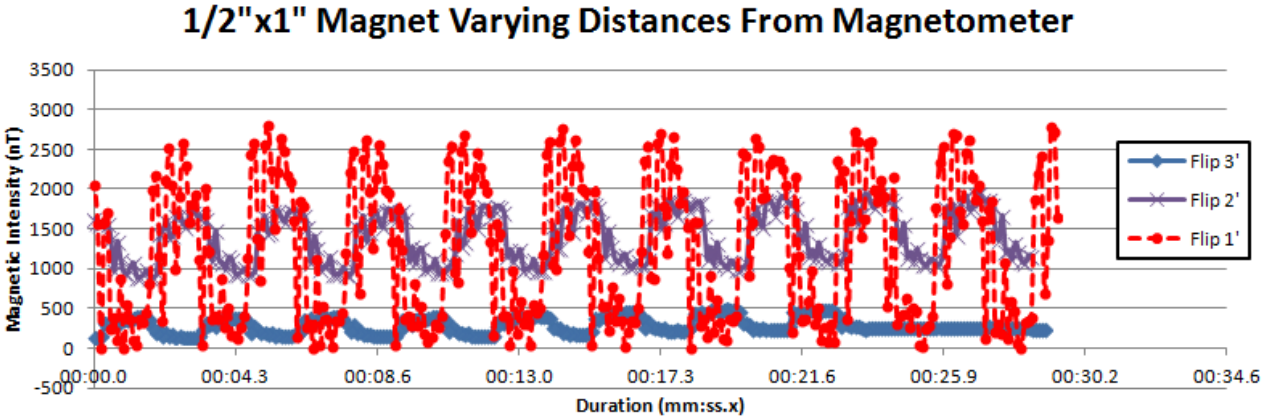

Fig. 6 Comparison of varying distances between a flipping smart rock and the magnetometer

It was also discovered that the alternating current coil system can easily be integrated into the current active smart rock board with magneto-inductive communication without affecting the capabilities of the active smart rock. This allows for a potential fusion of both active smart rocks within one system, allowing for additional redundancy and reliability of the overall monitoring system.

Task 2.2(a) Magneto-Inductive Communications – Engineering Design and Validation of Magneto-Inductive Transponders Submitted

Active Smart Rock - RSSI Processing Development of a localization scheme for the active Smart Rock system began during this quarter. Typically triangulation schemes are used for localization of a source by proceeding phase difference/time difference of arrival at multiple

receiving nodes. However, with the magneto-inductive communication link used in Smart Rock system, these methods cannot be used due to low frequency of operation – 125 KHz, which results in large wavelength equal to 2.4 km. Small meter-scale distance changes will not be observable at a typical Smart Rock localization/bridge site. Therefore, Received Signal Strength Indication (RSSI) data at multiple receiver nodes is proposed in this study. The Smart Rock electronic boards are equipped with Low-Frequency receiver IC AS3930 capable to sense RSSI. The sensitivity of AS3930 RSSI was tested. Figs. 7 and 8 show an Agilent A5181A analog signal generator and a Smart Rock PCB with AS3930 IC onboard, respectively. The output cable from the signal generator is connected to the receiver IC input pins.

Fig. 7 Agilent A5181A signal generator

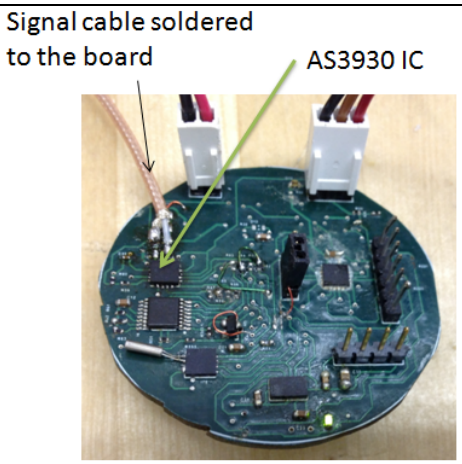

Fig. 8 Smart rock PCB

Continuous sinusoidal signal with 125 KHz frequency was used during the tests. The RSSI readings were processed by a PIC microcontroller through SPI bus connection and transmitted to the Base Station by the connected loop antenna. The observed input voltage range for RSSI estimation is [44:43000] uVrms.

The RSSI register at AS3930 provides 5 bits value. Each step corresponds to 2 dB. Figs. 9 and 10 compare the datasheet information and the observed IC behavior. The tested IC demonstrated a good correlation with the datasheet, validating the RSSI reading range and embedded software routines for data processing.

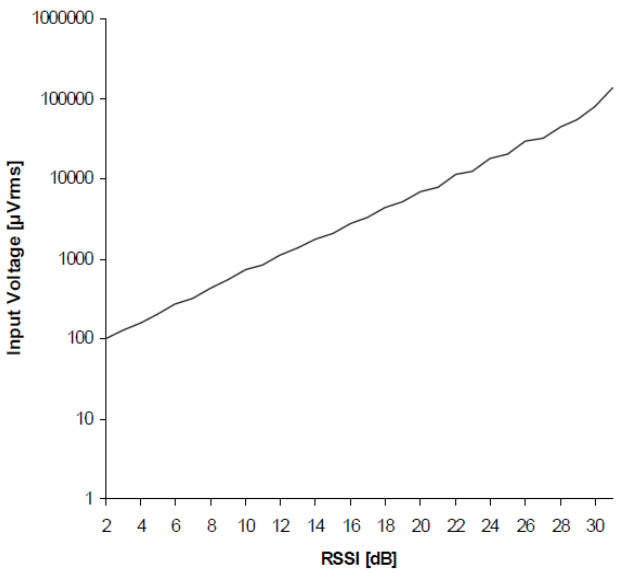

Fig. 9 Datasheet graph

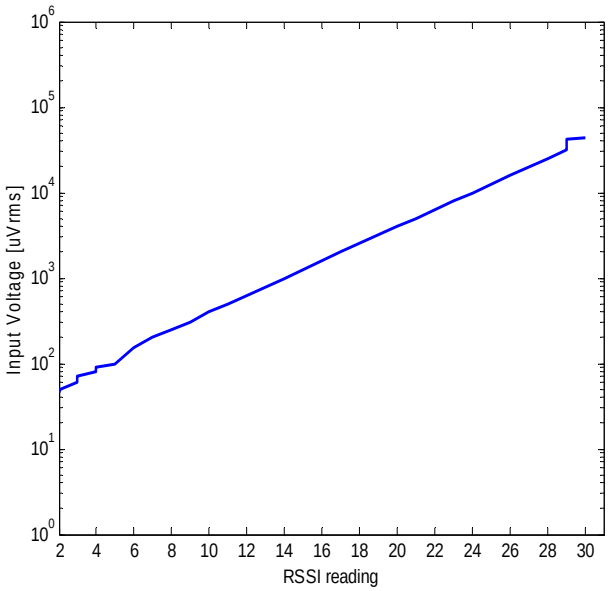

Fig. 10 Experimental graph

The actual dynamic range of the AS3930 RSSI reader is ~60 dB. It provides very good low-signal sensitivity (~43 uV, one of the best compared to similar chips), but has limited maximum input voltage – 43 mV only. This could be too low for inter-rock communication at near distance, thus adding more demand on the fine tuning of antennas for very good receptions.

The dynamic range of RSSI reader can be extended by adding a second RSSI-reader circuitry to the Smart Rock electronic board. Further experimental tests with rock-to-rock communication will be performed in April 2013 for best strategy development.

Flipping Magnet circuitry To support the development of a controllable magnet active smart rock system, the Smart Rock electronic circuitry was used with a magnetic flipping core. A special extension board based on H-bridge component was designed and connected to the Smart Rock v3 PCB through the free pins on the PIC microcontroller.

The controllable magnet active smart rock unit was demonstrated to be fully functional. It can be woken up by an external RF signal with a pre-programmed scenario. Figs. 11 and 12 show photo of the laboratory setup with a flipping magnet unit and the current-controlling circuitry block scheme, respectively.

Input A and Input B of the H-Bridge are connected to the PIC microcontroller Input/Output pins. As indicated in Fig. 12, the H-Bridge has power line connection and two outputs – Output A and Output B. A coil and resistive load (for current limiting purposes) is connected to the H-bridge output. When current passes through the coil, a relatively strong magnetic field is generated within the coil core. Figs. 13-15 show the coil model and magnetic field distribution inside a coil.

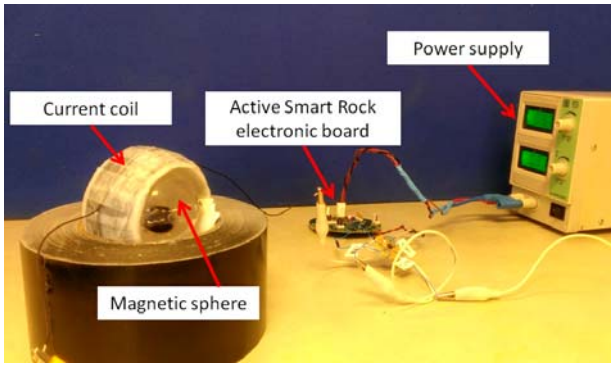

Fig. 11 Flipping magnet extension connected to Smart Rock v3 PCB

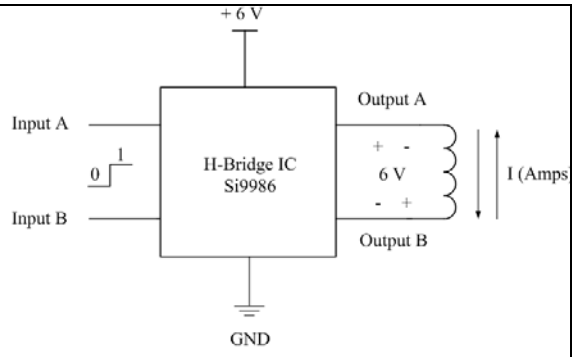

Fig. 12 Flipping magnet extension circuitry

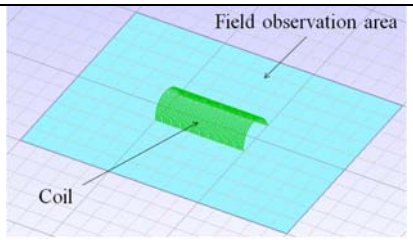

Fig. 13 Simulation model of a solenoid coil driven by a current source

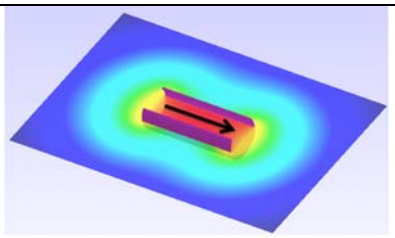

Fig. 14 Magnetic field distribution and direction within the coil

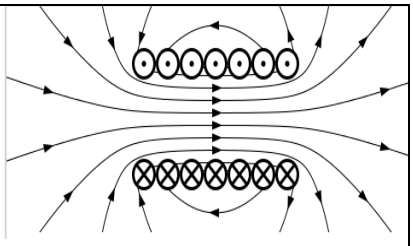

Fig. 15 Magnetic field distribution and direction within the coil

The generated field strength depends on the number of turns in the coil, coil dimensions and passing current magnitude. The “frictionless and free to move” magnet placed within the coil will be aligned with the magnetic field vector, which is co-oriented with a coil axle. If the direction of current flow is altered, the magnetic field vector will flip, forcing the magnet to move.

With the tested magnetic spheres, the current consumption required for effective flipping of the magnet is 0.3 A. The active Smart Rock system uses up-to 1 A current for magneto-inductive communication link with the coil-antenna RF transmission, thus magnet flipping circuitry does not require any additional power source or power distribution system redesign and is compatible with the current state Smart Rock electronic circuitry.

New Analog Filter / Preamplifier / Demodulator design The Digital Signal Processing (DSP) routines were implemented on a DSP board. However, the system had limited carrier frequencies that are acceptable in Audio frequencies range. Therefore, a new Base Station module has been designed with frequency shifting functionality and improved filtering, amplification and analog demodulator circuitry. Fig. 16 shows a block-diagram of the new analog pre-amplifier unit.

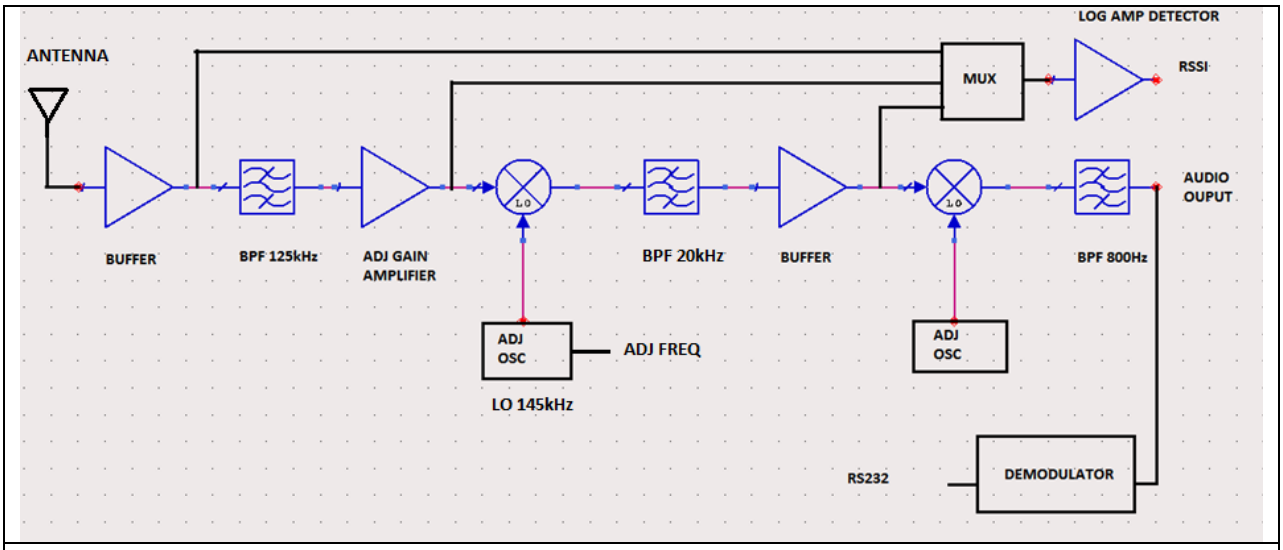

Fig. 16 New base station preamplifier module block-diagram

The input end was connected to the 125 KHz antenna; the received signal was passed through a band-pass-filter with low bandwidth, and then amplified and mixed down to 20 KHz at the next stage. Next, one more stage of frequency shift was performed to produce output at 800 Hz frequency, which is compatible with the originally developed DSP routines. The RSSI estimation is available at three stages – original signal and two intermediary steps, providing better dynamic responses of the complete system. The module also features a demodulator, generating standard RS232 output.

The audio output signal can be then connected to any computer sound card and easily loaded into Matlab / Lab View or any other similar toolkits with signal processing capabilities. Fig. 17 shows a layout and control components placement scheme for the new base station preamplifier PCB. The boards were currently in production phase and will be available for future tests.

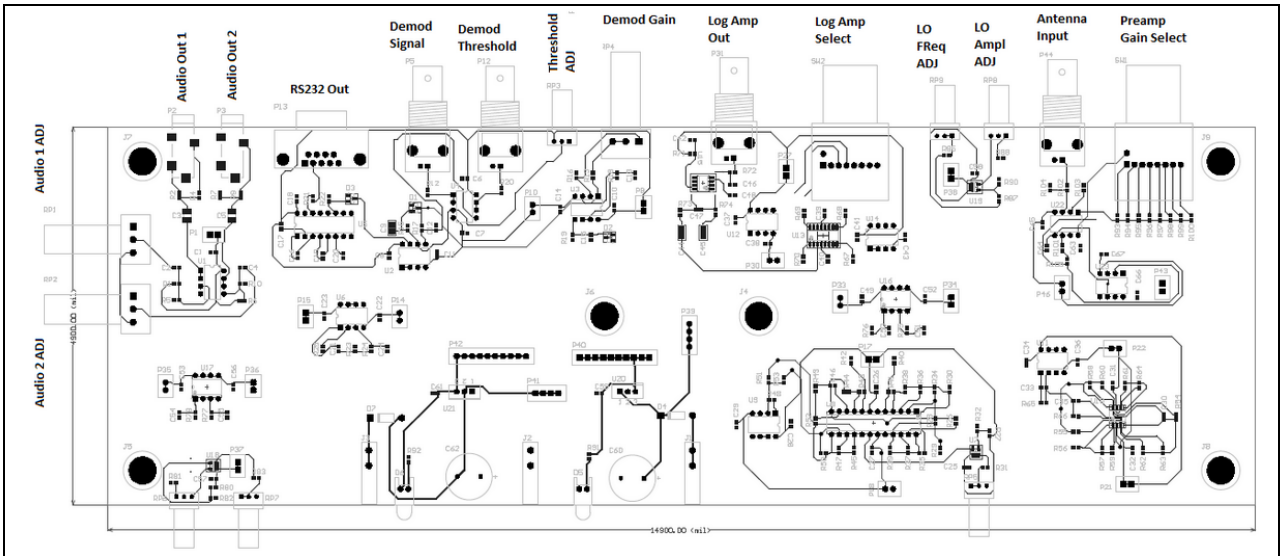

Fig. 17 New base station preamplifier module layout

Task 2.2(b) Acoustic Communications – Engineering Evaluation of Acoustic Communication Systems for Bridge Scour Monitoring

In this quarter, the localization method using Time Difference of Arrival (TDoA) has been thoroughly investigated with simulations and tests in field condition. The transmitter consisted of a C6713 board, a digital to analog converter (DAC), a power amplifier and an acoustic projector. The receiver consisted of two channels of hydrophones, a bandpass filter, a low-noise amplifier (LNA), and an analog-to-digital converter (ADC), all interfacing with the C6713 board. The experiment was performed in the pond of Lions Club Park, Rolla, MO, as shown in Fig. 18. The water temperature was measured to be T = 5 °C, the speed of sound in water was calculated as c = 1426 m/s according to the empirical formula, the bit rate was set to R= 5000 bps, and thus the range resolution is 0.2852 m/bit.

Fig. 18 Test site in the pond of Rolla Lions Club Park (Rx-Tx separation = a few meters due to limited power amplification)

The relative locations of the projector and hydrophones are shown in Fig. 19, where the distance between Hydrophone-1 and Projector as d_1 and the distance between Hydrophone-2 and Projector as d_2. Therefore, their distance difference $d_{12} = d_1 - d_2 = 2.13$ m. Since the On-Off Keying (OOK) modulation was used in the communication system, bit 1 is represented by a cosine wave of frequency fc=125 kHz, and bit 0 is represented by DC voltage. When transmitting one OOK pulse, the received pulses at the two hydrophones indicate TDoA clearly, as shown in Fig. 20. When transmitting a 63-bit maximum-length pseudo-noise (PN) sequence and 8 payload bits repeatedly, we can use the correlation property of the pulse to automatically detect the start of the data block. The received pass-band signals at the two hydrophones are shown in Fig. 21.

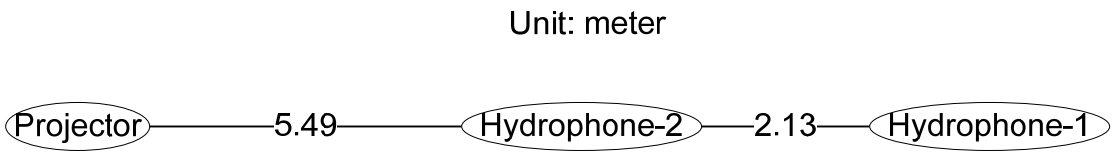

Fig. 19 Relative locations of the projector and hydrophones

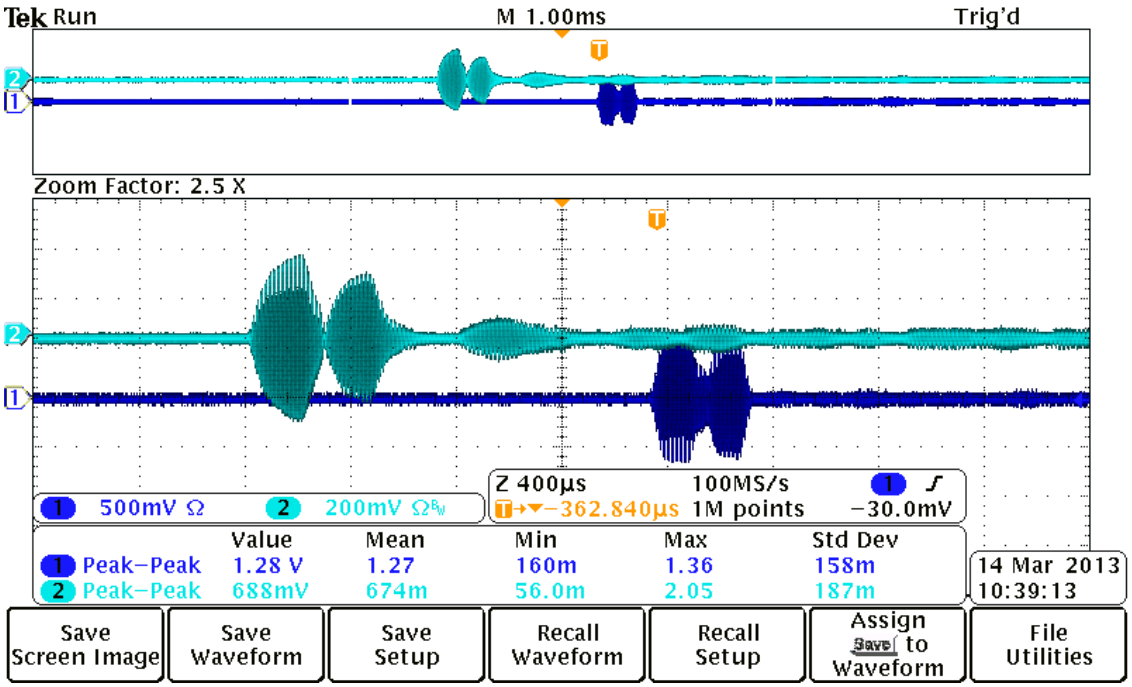

Fig. 20 The received oscilloscope waves at the two hydrophones when transmitting one OOK modulated pulse at the projector

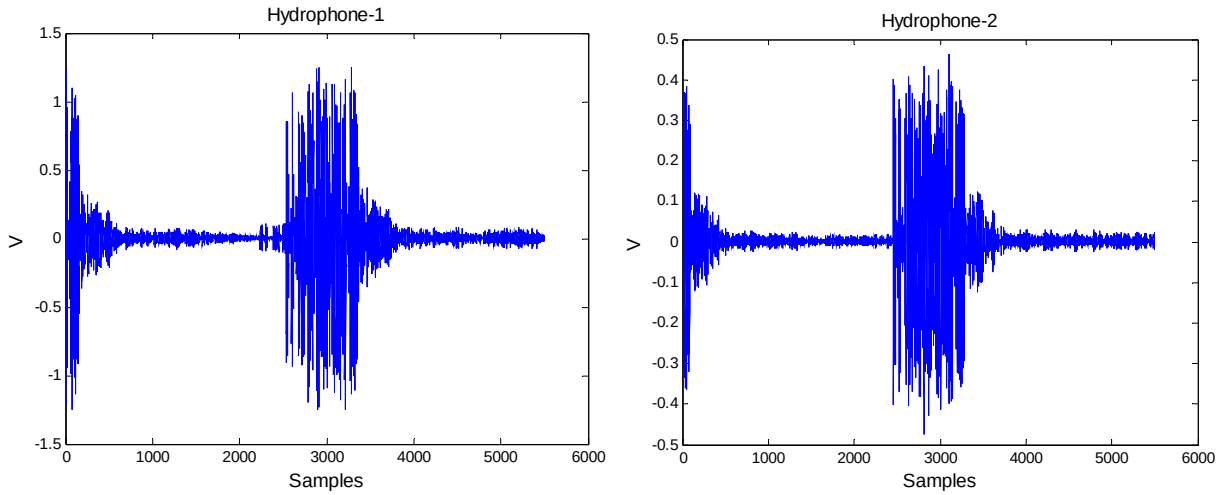

Fig. 21 The received bandpass signals at the two hydrophones when transmitting the 63-bits maximum length PN-sequence and 8 payload bits

The C6713 DSP at the receiver processed the 2-channel signals simultaneously, and calculated the distance difference d_{12} and bit error rate (BER). Table 1 shows the range measurement and BER performance for five frames. The accuracy of the measured distance difference is 0.05 m, while the BER performance is affected by strong acoustic reverberation, indicating that channel equalization is required for improved data detection.

Table 1 Distance difference d_{12} using TDoA and corresponding BER performance

Frame	d_{12} (m)	BER at Hydrophone-1	BER at Hydrophone-2
1	2.18	0.114	0.253
2	2.18	0.038	0.164
3	2.15	0.05	0.152
4	2.18	0.05	0.17
5	2.18	0.076	0.165

When multiple DSP receivers are required for field deployment, for example, at both sides of a river, timing synchronization among the receivers is critical to the TDoA localization method, as illustrated in Fig. 22. Several options for the timing synchronization of multiple receivers has been researched and simulated. For this study, a commercial GPS timing module is integrated into each DSP receiver.

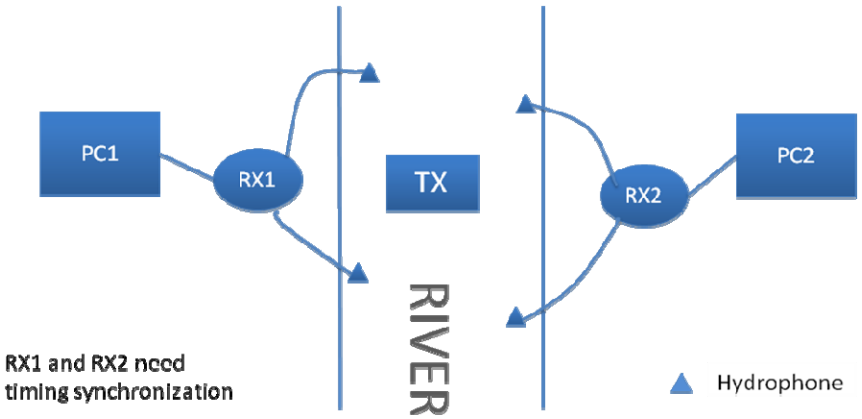

Fig. 22 Timing synchronization approach for localization

While waiting for the order to come in, we emulated the 1PPS (pulse-per-second) output of the GPS timing module by a signal generator and changed original DSP receiver interfaces. Fig. 23 shows the hardware setup for the new solution of timing synchronization. The 1PPS signal from Arbitrary Signal Generator triggered the DSP as an external interrupt. The DSP then generated the 55 kHz sampling signals for ADC. This solution encounters minimal changes made to the original hardware

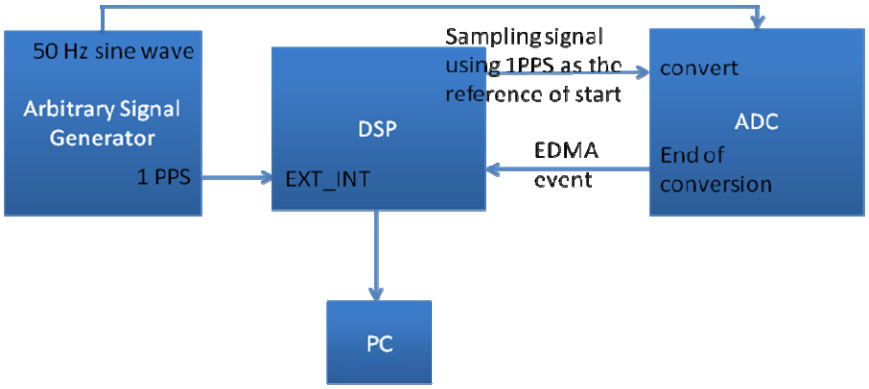

Fig. 23 Hardware setup for the simulation of timing synchronization

Other peripherals of the acoustic transmitter and receiver circuits were also refined, including the power amplifiers and match network at the transmitter, the low noise amplifier and band-pass filter at the receiver, the power supplies for both transmitter and receiver. Both transmitter and receiver hardware setups are now thoroughly tested in laboratory.

Task 3.2 Field Validation Planning and Execution – Field Test Plan and Data Analysis Submitted

Field monitoring with the previously deployed smart rocks continued. The results will be reported towards the end of this project.

I.2 PROBLEMS ENCOUNTERED

There are no problems encountered in this quarter. However, the project continued to be delayed for about three months as explained in the previous report. On the other hand, the project expenditure is in general agreement with the project progress.

I.3 FUTURE PLANS

Three subtasks will be executed during the next quarter. A brief description of various activities in each subtask is described below:

Task 1.1 Design, fabricate, and test in laboratory and field conditions DC magnetic sensors with embedded magnets aligned with the earth gravity field. Summarize and document the test results and the performance of passive smart sensors.

The field test data collected at bridge sites in late summer, 2012, will be further analyzed to demonstrate the effectiveness of a simple localization scheme following the triangulation strategy. In addition, the field performance of passive smart rocks will continue to be monitored in the following quarters.

Task 1.2 Research, summarize, and document the degree of potential steel interferences to magnetic measurements. Investigate ways to compensate the interference effect and develop a rock localization technique.

Further tests will be conducted in laboratory to characterize how adjacent metals affect the magnetic field measurement.

Task 2.1 Design, fabricate, and test in laboratory and field conditions active smart rocks with embedded controllable magnets or with embedded electronics. Summarize and document the test results and the performance of active smart rocks.

Further development of the controllable magnet active smart rock will be conducted to improve the efficiency of the flipping system and in turn reduce the necessary energy to run the system. It has been proposed to modify a typical gyroscope to reduce the overall friction effect further as well as fix the orientation of the coil in the optimal position for system efficiency. In theory by installing the coil along the outer gimbal as illustrated in Fig. 24, weighting one side to constantly orient to gravity (essentially like balancing a tire), and modifying the inner gimbal to hold the passive smart rock, the power required to overcome the friction will be reduced and the orientation of the system will be consistently with respect to gravity.

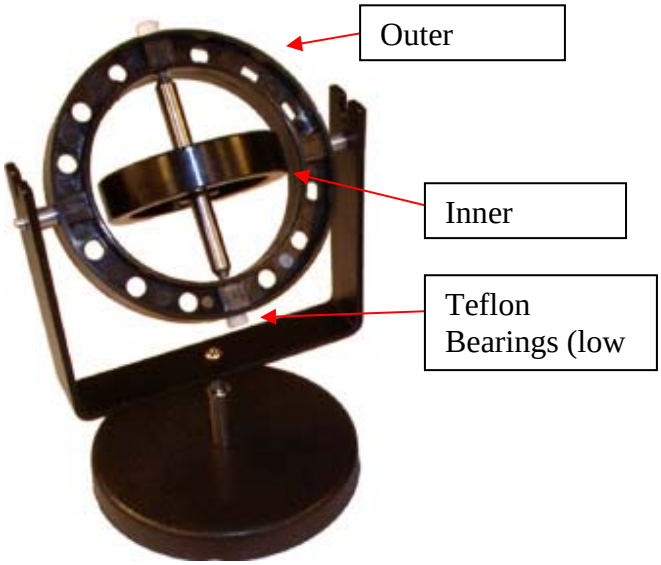

Fig. 24 Gyroscope for the proposed controllable magnet active smart rock

Task 2.2(a) Design, fabricate, and test in laboratory and field conditions magneto-inductive transponders. Summarize and document the test results and the performance of transponders.

Further development activities include:

- Long-term monitoring of Smart Rocks installed at two bridge sites (reported previously)
- Inter-rock communication arrangement
- Development of new localization schemes using inter-rock RSSI data
- New base station unit assembly

- Optimization of the magnet flipping circuitry
- Implementation of commands protocol to Smart Rock sensors remote reconfiguration
- Gyroscope data processing for movement trajectory recovery tests

Task 2.2(b) Research, summarize, and document current underwater acoustic transmission practices and required modifications for bridge scour monitoring.

Both transmitter and receiver programs have been thoroughly tested and optimized. In the remaining performance period, the following tasks will be performed, including:

1. Develop the detection method for TDoA using four channel receiver
2. Develop the localization algorithm using TDoA
3. Test the TDoA method and the localization algorithm in field experiment
4. Integrate the DSP transmitter with sensor board and micro-controller
5. Integrate transmitter and receiver together and develop power management circuits.

Task 3.2 Plan and execute the field validation tasks of various prototypes. Analyze the field performance of smart rocks and communication systems.

Initial field tests at two bridge sites were completed. The field test data will be further processed to evaluate the field performance of various technologies.

II – BUSINESS STATUS

II.1 HOURS/EFFORT EXPENDED

The planned hours and the actual hours spent on this project are given and compared in Table 2. In the seven quarter, the actual hours are more than the planned hours. However, the actual cumulative hours are approximately 77% of the planned hours, corresponding to the project delay starting the third quarter. The cumulative hours spent on various tasks by personnel are presented in Fig. 25.

Table 2 Hours spent on this project

	Planned		Actual	
	Labor Hours	Cumulative	Labor Hours	Cumulative
Quarter 1	752	752	184	184
Quarter 2	752	1504	345	529
Quarter 3	752	2256	381	909
Quarter 4	752	3009	166	1075
Quarter 5	720	3729	721	1877
Quarter 6	720	4449	1069	2946
Quarter 7	720	5169	1006	3952

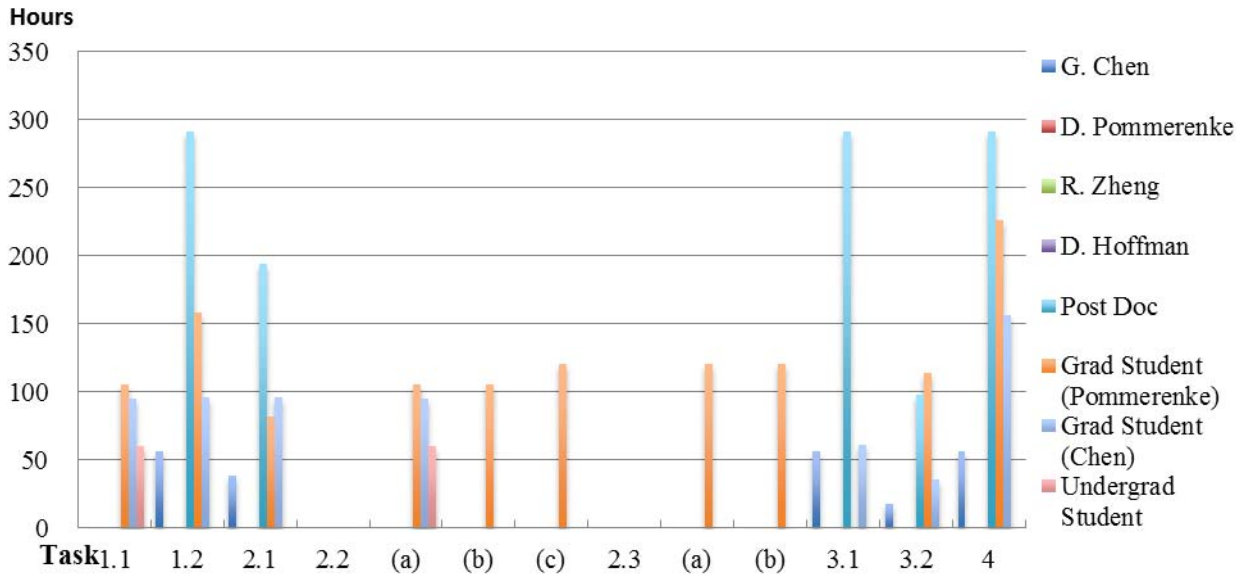

Fig. 25 Cummulative hours spent on various tasks by personnel

II.2 FUNDS EXPENDED AND COST SHARE

The budgeted and expended RITA funds accumulated by quarter are compared in Fig. 26. Approximately 58% of the budget has been spent till the end of seven quarter. During the seven quarter, 84% of the budget has been spent. Therefore, the project expenditure in the seven quarter is in alignment with the budget. The actual cumulative expenditures from RITA and Missouri S&T/MoDOT are compared in Fig. 27. The expenditure from RITA is significantly less than the combined amount from the Missouri S&T and MoDOT.

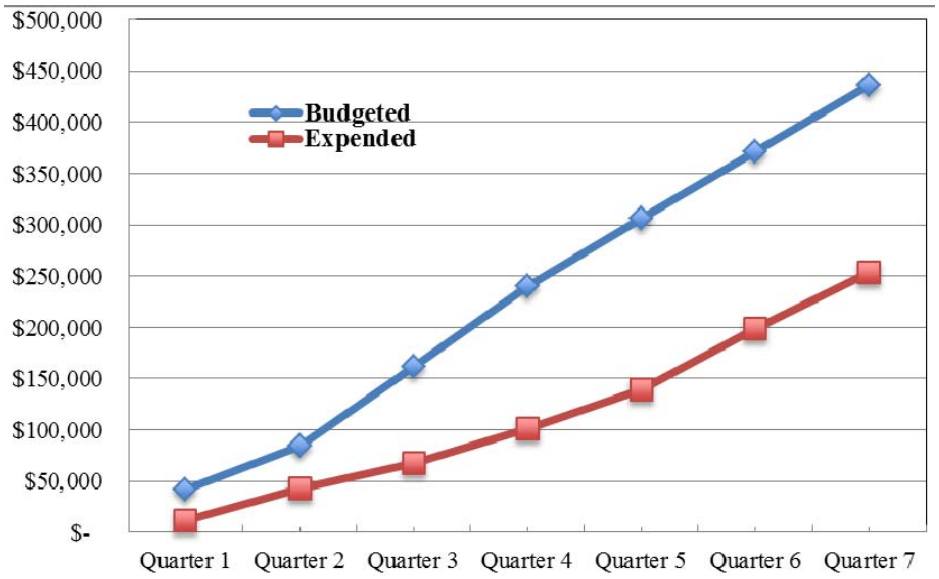

Fig. 26 Comparison of RITA budget and expenditure accumulated by quarter

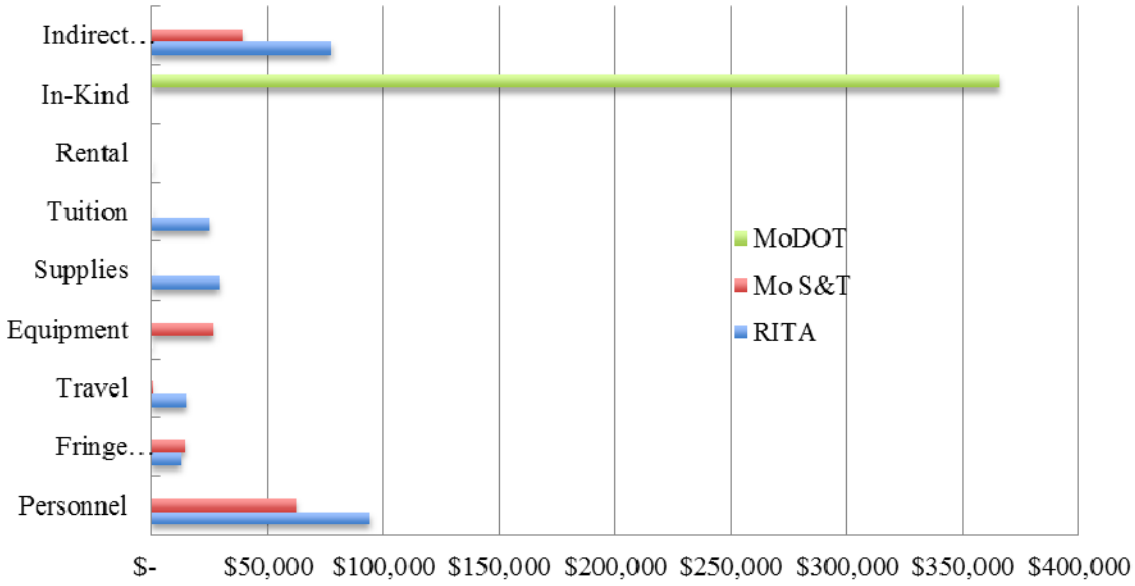

Fig. 27 Cummulative expenditures by sponsor